ACS OMEGA

http://pubs.acs.org/journal/acsodf

Article

3′-Sulfo-TF Antigen Determined by GAL3ST2/ST3GAL1 Is Essential for Antitumor Activity of Fungal Galectin AAL/AAGL

Yang Li, Yan Li, Jing Xia, Qing Yang, Yijie Chen,* and Hui Sun*

Cite This: *ACS Omega* 2021, 6, 17379−17390

Read Online

ACCESS | Metrics & More | Article Recommendations | Supporting Information

ABSTRACT: Many lectins have been reported to have antitumor activities; identifying the glycan ligands in tumor cells of lectins is crucial for lectin clinical application. An edible mushroom galectin, *Agrocybe aegerita* lectin (AAL/AAGL), that has a high antitumor activity has been reported. In this paper, based on the glycan array data, it is showed that the Thomsen-Friedenreich antigen (TF antigen)-related *O*-glycans were found to be highly correlated with the antitumor activity of AAL/AAGL. Further glycosyltransferase quantification suggested that the ratio between GAL3ST2 and ST3GAL1 (GAL3ST2/ST3GAL1), which determined the 3′-sulfo-TF expression level, was highly correlated with the antitumor activity of AAL/AAGL. Overexpressing the enzyme of GAL3ST2 in HL60 and HeLa cell lines could increase the growth inhibition ratio of AAL/AAGL from 22.7 to 43.9% and 27.8 to 39.1%, respectively. However, ST3GAL1 in Jurkat cells could decrease the growth inhibition ratio from 44.7 to 35.6%. All the data suggested that the 3′-sulfo-TF antigen is one of the main glycan ligands that AAL/AAGL recognizes in tumor cells. AAL/AAGL may potentially serve as a reagent for cancer diagnosis and a targeted therapy for the 3′-sulfo-TF antigen.

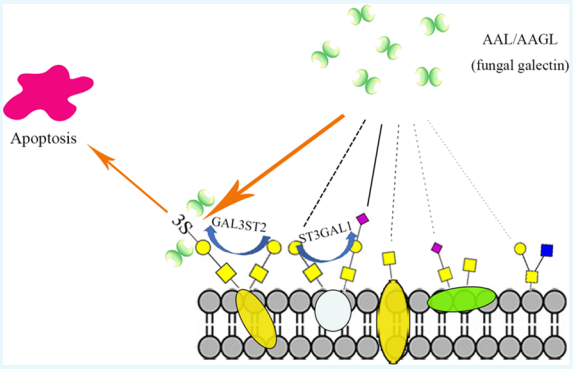

1. INTRODUCTION

Lectins, also known as glycan-binding proteins, are a group of carbohydrate-binding proteins of nonimmune origin that are ubiquitously distributed in plants, animals, and fungi and have multiple significant biological functions, such as antifungal, antiviral, and, most notably, antitumor activities.[1−3] These antitumor lectins are known to possess proinflammatory, antiproliferative, antimicrobial, immunomodulatory, and antiviral activities by being involved in growth regulation, cell adhesion, cell migration, cell apoptosis, and immune responses.[4−6]

Several lectins have been investigated for their anticancer effects in preclinical and clinical stage trials.[7] For example, intravenous treatment with Concanavalin A (ConA) has been used to induce in vivo autophagic cell death in hepatoma cells in a murine in situ hepatoma model.[8] A diet containing *Phaseolus vulgaris* agglutinin (PHA) was demonstrated to dramatically reduce the growth of an established murine non-Hodgkin lymphoma tumor in mice.[9] Mistletoe lectin has been reported to exhibit potent inhibition of tumor growth and metastasis through apoptosis in melanoma and ovarian cancer.[10] The in vivo anticancer efficiency of Abrus agglutinin (AGG) has been evaluated in several tumor models through the induction of cell death and activation of Th1 immunomodulation.[11] AGG treatment significantly reduced the growth of HCC in nude mice bearing HepG2 xenografts, efficiently suppressed human breast tumor growth in nude mice, inhibited the growth of tumors in a FaDu xenograft model, targeted cancer stem-like cells by eliminating their self-renewal capacity and EMT, and had antitumor activities in colorectal cancer.[12] Intraperitoneal injection of *Momordica charantia* lectin has been reported to result in a suppression of approximately 45% in the growth of nasopharyngeal carcinoma xenograft tumors that had been inoculated subcutaneously in nude mice, leading to the induction of apoptosis in cancer cells.[13] *Ricinus communis* agglutinin I (RCA I), a galactose-binding lectin, showed anticancer therapeutic activity by targeting tumor blood vessels, which led to a reduction in the expression levels of VEGFR-2 and tumor regression.[14]

There are two plant lectins in clinical stage trials. *Viscum album* lectin extract intratumoral injections in 123 colon adenoma cancer patients produced results with complete success, without adverse or life-threatening drug reactions[15] and a complete regression in a 78-year-old Caucasian male.[16] The combinatorial treatment of *Viscum album* L. lectin with different standard anticancer drugs resulted in improved one-year and three-year overall survival rates in stage IV nonsmall cell lung cancer patients.[17] Mistletoe lectin ps76a2 improved

Received: March 23, 2021
Accepted: June 4, 2021
Published: July 1, 2021

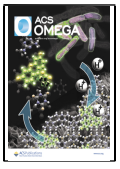

https://doi.org/10.1021/acsomega.1c01544
ACS Omega 2021, 6, 17379−17390

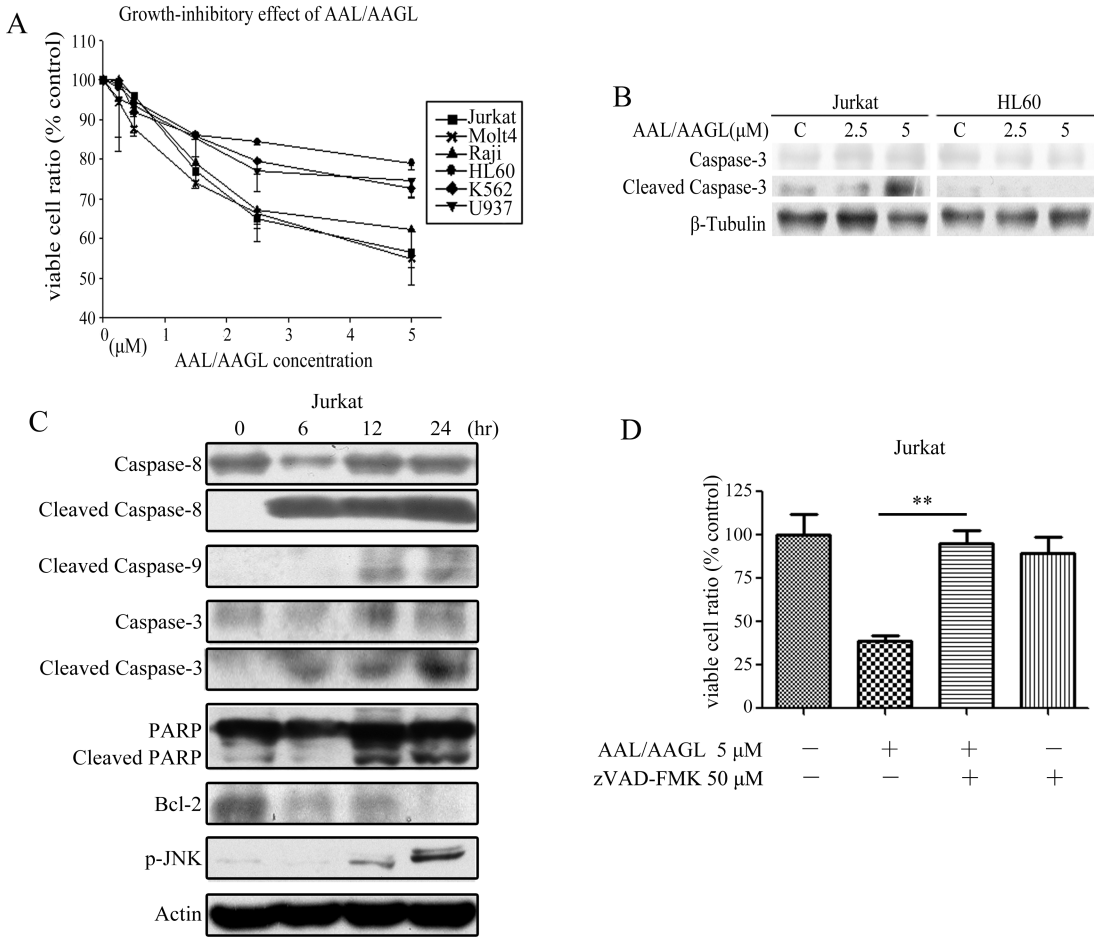

Figure 1. Different antitumor effects of AAL/AAGL in several tumor cells. (A) Different concentrations of AAL/AAGL incubated with six types of tumor cells for 48 h, after which the growth inhibition rate was assessed with a CCK-8 kit. (B) Jurkat and HL60 cells were treated with AAL/AAGL (2.5 and 5 μM) and PBS, and the expression level of caspase-3 was detected by the Western blot after 48 h. (C) Jurkat cells were treated with 5 μM AAL/AAGL, and the cells were collected after 6, 12, and 24 h, respectively. The expression levels of cleaved caspase-8, 9, 3, cleaved PARP, Bcl-2, and p-JNK were detected by the Western blot. (D) Jurkat cells were treated with 5 μM AAL/AAGL and 50 μM zVAD-FMK, a caspase inhibitor. After 48 h, the inhibition rate in Jurkat cells in each group was assessed with a CCK-8 kit.

the quality of life of breast cancer patients during chemotherapy.[18]

Most of these antitumor activities are directly related to the ability of these proteins to interact with carbohydrates via the carbohydrate recognition domain (CRD).[19,20] Numerous lectins have been studied in great detail to unravel their carbohydrate-binding specificity by using glycan inhibition assays; frontal affinity chromatography and glycan microarrays.[21,22] Glycan microarrays are a high-throughput method to determine the specificity of glycan-binding proteins. In addition, the glycan array technology also allows quantification of the relative affinity of carbohydrate-binding proteins to glycans.[23] The specific binding of a lectin to a carbohydrate structure can be exploited in lectin affinity chromatography for glycan enrichment.[24] It is well known that ConA is a mannose binding lectin, soybean agglutinin (SBA) is specific to the galactosylated ligand,[25] and *Phaseolus vulgaris* lectin (PHA-E) has an unusual specificity toward biantennary galactosylated N-glycan with bisecting *N*-acetylglucosamine (GlcNAc).[26] ConA is now the most widely used lectin for the characterization and purification of high-mannose N-glycan-containing glycoconjugates and for the detection of these carbohydrate structures on biomolecules and cells.[20] Even though several glycoprotein ligands of SBA, ConA, and PHA have been identified, such as SBA interacting with TLR4, ConA, TLR2/6 and PHA, TLR2/6, 4, and 5, the detailed carbohydrate moiety in these glycoprotein ligands recognized by these antitumor lectins on the tumor cell membrane surface has not been specifically identified.[27]

AAL/AAGL, a lectin purified from the edible mushroom *A. aegerita*, is an antitumor protein that exerts its tumor-suppressing function via apoptosis-inducing activity in cancer cells. AAL/AAGL belongs to the galectin family, which has conserved the CRD of the galectin family and β-galactoside binding activity.[28] It was reported that AAL/AAGL can be internalized by recognizing the carbohydrate moiety on the cell membrane surface and localizes in the nucleus of HeLa cells similar to human galectins.[29,30] Moreover, the apoptosis-inducting activity is closely related to the nuclear localization. Crystallization of AAL/AAGL and the tumor Thomsen-Friedenreich antigen (TF antigen) also indicated that AAL/AAGL could bind to the TF antigen just as observed for other mammalian galectins.[31] However, the specific ligand that determines the antitumor activity of AAL/AAGL has still not been illuminated.

In this study, we demonstrated that the antitumor activity of AAL/AAGL was triggered by the interactions with carbohydrate molecules on the cell surface. By analyzing the glycan

https://doi.org/10.1021/acsomega.1c01544
ACS Omega 2021, 6, 17379−17390

array data of AAL/AAGL and its mutants, we found that the 3′-sulfo TF and 3′-sialyl-TF antigen had the highest binding for AAL/AAGL among the TF-related antigens. Further investigation indicated that the expression level of the 3′-sulfo-TF antigen determined by the ratio of GAL3ST2/ST3GAL1 had a high correlation with the antitumor activity of AAL/AAGL. These data suggested that AAL/AAGL could be proposed as a drug for targeting tumor cells that strongly express 3′-sulfo-TF antigens.

2. RESULTS

2.1. Antiproliferative Effect of AAL/AAGL through the Induction of Apoptosis In Vitro. In our previous papers, a series of experiments indicated that AAL/AAGL possesses a potent antitumor function in several tumor cell lines, including HeLa, SW480, and SGC-7901 cells, and apoptosis-inducing activity in tumor cells.[32] In this paper, several leukemic cell lines (including Jurkat, Molt4, HL60, and K562 cells) and two kinds of lymphoma cell lines (Raji and U937 cells) were used for testing the antitumor activity of AAL/AAGL. As shown in Figure 1A, AAL/AAGL displayed a growth-inhibitory effect in a time-dependent and concentration-dependent manner (Table 1). Jurkat, Molt4, and Raji cells were more sensitive

Table 1. Effect of 5 μM AAL/AAGL on the Viable Cell Ratio and Growth Inhibition Rate of Cells

cells	viable cell ratio (% control)	growth inhibition (%)
Jurkat	56.37 ± 3.63	43.63 ± 3.63
Molt4	54.00 ± 8.86	46.00 ± 8.86
Raji	62.19 ± 5.35	37.81 ± 5.35
HL60	78.94 ± 1.74	21.06 ± 1.74
K562	72.54 ± 2.00	27.46 ± 2.00
U937	74.60 ± 4.30	25.40 ± 4.30

to AAL/AAGL compared with HL60, K562, and U937 cells. To further detect the sensitivity of different cells to AAL/AAGL, we selected Jurkat cells, which were more sensitive to AAL/AAGL, and investigated the activation of apoptosis signals after AAL/AAGL treatment. In Figure 1B, Jurkat and HL60 cells were selected as sensitive and nonsensitive cells, respectively, for further analysis. AAL/AAGL activated caspase-3 in Jurkat cells but not in HL60 cells after AAL/AAGL treatment for 48 h. As shown in Figure 1C, treatment of AAL/AAGL-sensitive Jurkat cells with AAL/AAGL showed that the protein expression levels of caspase-8, −9, −3, and PARP were upregulated, the JNK MAP kinases were activated, and the expression of Bcl-2 was downregulated. The blockade of caspase activation by the pretreatment with Z-VAD-FMK, a pan-caspase inhibitor, prevented the cell death induction by AAL/AAGL in Jurkat cells (Figure 1D). Taken together, these data suggest that Jurkat, Molt4, and Raji cells are more sensitive to AAL/AAGL, compared with HL60, K562, and U937 cells and that AAL/AAGL induces apoptosis in Jurkat cells in a caspase-dependent manner.

2.2. Antitumor Activity of AAL/AAGL Is Directly Proportional to Cell Surface Binding Activity. To explore the reason for the sensitivity differences to AAL/AAGL between the different tumor cells, we investigated the cell binding of AAL/AAGL in these cells. As shown in Figure 2A, the cell lines with a stronger binding for AAL/AAGL were more sensitive to AAL/AAGL, and HL60, which was resistant to AAL/AAGL, had the lowest binding for AAL/AAGL (Figure 2A,B). By analysis and statistics of the linear regression method, a correlation value of 0.9646 was calculated between the binding of AAL/AAGL to different cells and the inhibition of AAL/AAGL-induced apoptosis in tumor growth (Table 1). The high correlation value indicated a very good fit of the linear regression line to the data points in Figure 2C. These results indicated that there is a high positive correlation between the cell surface AAL/AAGL binding and the antitumor activity of AAL/AAGL.

2.3. The Antitumor Activity of AAL/AAGL Is Dependent on the *O*-Glycans of Tumor Cells. Next, we tried to determine the glycans related to the binding of AAL/AAGL for different cells and the apoptosis-inducing activity of AAL/AAGL. Galectins, a family of at least 15 β-galactoside-binding proteins, are involved in growth development, as well as in cancer progression and metastasis, and lactose is commonly used as an inhibitor of galectins in vitro. The addition of 100 μM lactose abrogated the antiproliferative activity of AAL/AAGL (Figure 3A), showing that AAL/AAGL-induced cell death required AAL/AAGL binding to saccharide ligands on the surface of the cells. As reported previously, several galectins, in particular galectin-1 and galectin-3, can recognize the TF antigen, and the crystal structure of AAL/AAGL, complexed with the TF antigen, was also reported. We used benzyl-α-GalNAc, an *O*-glycan synthesis inhibitor, to inhibit the O-glycosylation of *O*-glycans. As shown in Figure 3B, treatment of Jurkat cells with benzyl-α-GalNAc resulted in decreased AAL/AAGL binding to these cells. The mean fluorescence intensity of cells treated with benzyl-α-GalNAc decreased approximately 35% compared with the control (Figure 3C). The viable cell ratio was increased dramatically from 54.9 to 83% (Figure 3D). Treatment of Jurkat cells with benzyl-α-GalNAc resulted in a dramatic decrease in sensitivity to AAL/AAGL-induced cell death. The annexin V-positive PI-positive cell ratio was reduced dramatically from 45.7 to 12.4% (Figure 3E,F). These results indicated that elongated *O*-glycans on cell-surface glycoproteins regulate the cells' sensitivity to AAL/AAGL-induced cell death.

2.4. 3′-Sulfo-TF, 3′-Sialyl-TF, and TF Binding Activities Show a High Correlation with the Antitumor Activity of AAL/AAGL. The TF antigen and related *O*-glycans have been reported as binding ligands of many galectins. We get the glycan array data of AAL/AAGL and its mutants (Supporting data 1−6) from CFG (http://www.functionalglycomics.org/) by searching the lectin name "AAL," for further TF and related *O*-glycan binding activity analysis. In Figure S1, we analyzed the glycan array of AAL/AAGL at different concentrations using a dot plot method according to the terminal-glycans. Several main O- and N-glycotypes are also marked in Figure S1. As shown in Figure 4A, the TF-related glycans were further analyzed in detail. The glycan array results of three concentrations of AAL/AAGL showed that at concentrations of 100 and 200 μg/mL, AAL/AAGL had a high binding for the 3′-sulfo-TF and 3′-sialyl-TF antigens, and at 20 μg/mL, AAL/AAGL only had a high binding activity for 3′-sulfo-TF. As shown in Figure 4B, mutant I144G retained both 3′-sulfo-TF and 3′-sialyl-TF binding activities, H59Q only retained the 3′-sulfo-TF activity, and R63H lost both TF-related glycan-binding activities. Due to the high binding activity of sulfo- and sialyl-TF, the correlation between binding activity and apoptosis-inducing activity was analyzed by regression. As shown in Figure 4C,D, there was a high correlation between these activities, and the R values were

https://doi.org/10.1021/acsomega.1c01544
ACS Omega 2021, 6, 17379−17390

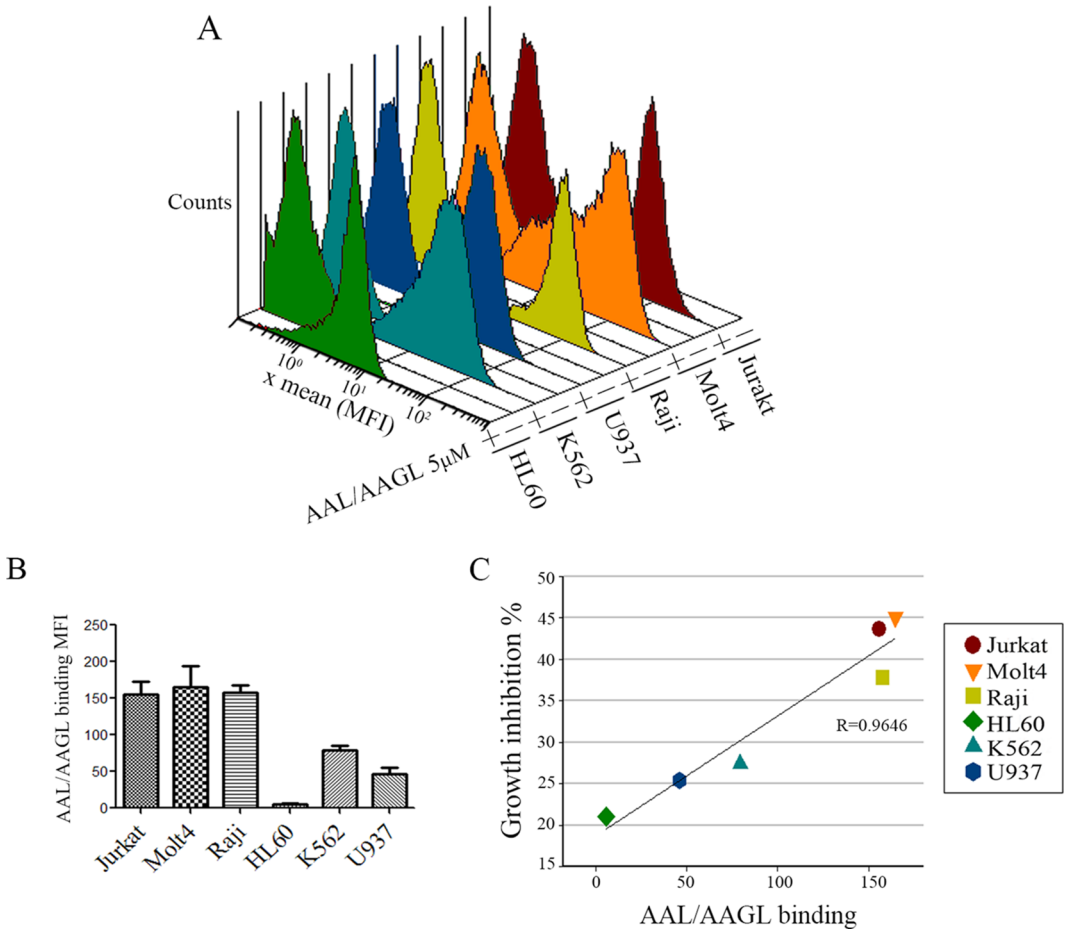

Figure 2. Antitumor activity of AAL/AAGL is directly proportional to cell surface binding activity. (A) Six kinds of cells were incubated with AAL/AAGL, and the binding of AAL/AAGL for the different cells was analyzed by flow cytometry. (B) ANOVA analysis of the data in Figure A. (C) Correlation analysis of the binding of AAL/AAGL for cells and tumor growth inhibition activity. The *R* value was shown to be 0.9646.

0.6657 and 0.5628 for 3′-sulfo-TF and 3′-sialyl-TF, respectively. However, there was a low correlation between TF and the apoptotic-inducing activity, with an R value of only 0.1779 (Figure 4E). The *R* value was 0.4034 between the lactose-binding ability of AAL/AAGL and its mutants and the apoptotic-inducing activity (Figure 4F). This has further indicated that AAL/AAGL-induced death in the sensitive cells is perhaps related to 3′-sulfo-TF and 3′-sialyl-TF.

2.5. Antitumor Activity of AAL/AAGL Has a Positive Relationship with GALST2/ST3GAL1 (Ratio between GAL3ST2 and ST3GAL1). According to the synthesis pathway of TF and related glycans (Figure 5A), there are five glycosyltransferases involved in the synthesis of these glycans. To identify which glycosyltransferases were the main factors determining the susceptibility to AAL/AAGL, all these five glycosyltransferases were quantified by RT-PCR and were analyzed for the correlation between their relative expression and antitumor activity.

The expression levels of the glycosyltransferase mRNA were normalized to GAPDH mRNA levels, and the expression levels of the glycosyltransferases in different cells were plotted against the inhibitory effect of AAL/AAGL. Linear regression analysis was then performed. As shown in Figure S2 and Table 2, there were low correlations between C1GALT1, C2GNT2, ST6GALNAC1, and inhibitory activity. We further investigated the expression of ST3GAL1 (Figure 5B) and GAL3ST2 (Figure 5C), which could transfer sialic acid and sulfate to the TF antigen, respectively. To our surprise, the correlation between the mRNA levels of these glycosyltransferases and inhibitory activity was also low (Figure 5B,C). These results indicated that a single glycosyltransferase may not determine the structure of the TF-related antigen and the binding of the cells for AAL/AAGL because sulfotransferases and sialyltransferases can compete for the same site of acceptors. The expression of 3′-sulfo-TF and 3′-sialyl-TF may depend on the ratio between sulfotransferases and sialyltransferases.

To confirm this hypothesis, the ratios between GAL3ST2 and ST3GAL1 were plotted against the inhibitory effects of AAL/AAGL, and the results showed that there was a high correlation between them. The R value calculated was 0.7807, which is the highest in the list in Table 2, compared with the other ratios between the glycosyltransferases of ST3GAL1/C2GNT1, GAL3ST2/C2GNT1, and inhibitory activity (Figure 5D−F). These results showed that the cells with a high ratio between GAL3ST2 and ST3GAL1 express more 3′-sulfo-TF antigens on the cell surface and that these cells are more sensitive to AAL/AAGL.

2.6. The Ratio between GAL3ST2 and ST3GAL1 Regulates the AAL/AAGL Sensitivity of Cells. To further confirm that the antitumor activity of AAL/AAGL was dependent on the 3′-sulfo-TF antigen, which was decided by the ratio between sulfotransferases and sialyltransferases, we regulated the ratio between GAL3ST2 and ST3GAL1 in three cell lines, including Jurkat cells, HeLa cells, and HL60 cells.

https://doi.org/10.1021/acsomega.1c01544
ACS Omega 2021, 6, 17379−17390

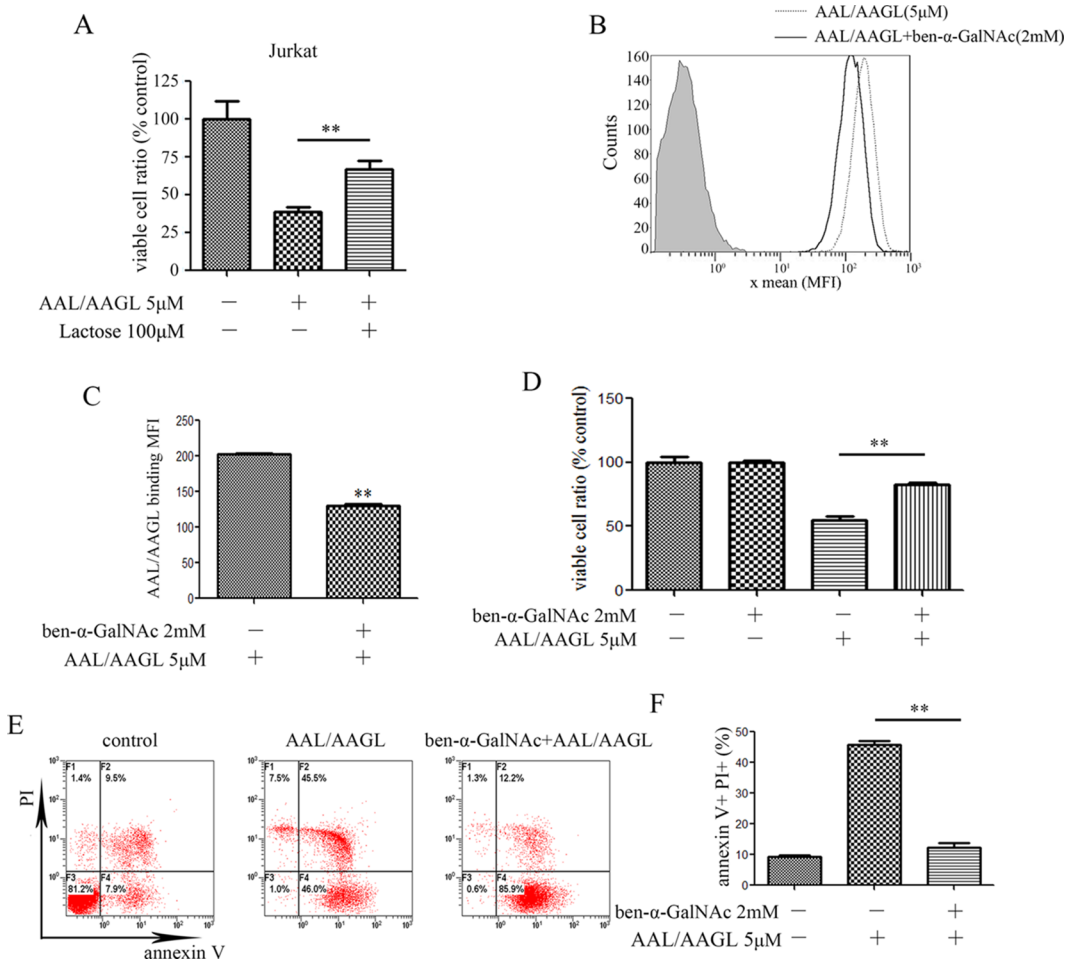

Figure 3. Antitumor activity of AAL/AAGL depends on the *O*-glycans on the cell surface. (A) Apoptosis was induced by the activity of glycan binding of AAL/AAGL. Jurkat cells were treated with 5 μM AAL/AAGL, and 100 μM lactose was added. After 48 h, the inhibition rate of Jurkat cells in each group was assessed with a CCK-8 kit. MFI: mean fluorescence intensity; (B) effects of benzyl-α-GalNAc treatment of Jurkat cells on the binding of AAL/AAGL for cells. Benzyl-α-GalNAc treatment of the Jurkat cells (solid line); untreated cells (dashed lines). Benzyl-α-GalNAc inhibited the addition of *O*-glycans, after which the AAL/AAGL binding rate was assessed by flow cytometry. (C) ANOVA analysis of the data in Figure 3B. (D) CCK-8 kit was used to assess the effect of benzyl-α-GalNAc and AAL/AAGL treatment in Jurkat cells on the viable cell ratio of the cells. (E) Influence of benzyl-α-GalNAc-treated Jurkat cells by an annexin V-PI double staining assay on the apoptosis induced by AAL/AAGL. (F) Statistical analysis of the data on the annexinV-PI+cell ratio in Figure 3E. $^{**}p < 0.01$.

The ST3GAL1 had been overexpressed in Jurkat cells. Because of the competition of GAL3ST2 and ST3GAL1 for the same site of the TF antigen, overexpressing ST3GAL1 in Jurkat reduced the 3′-sulfo-TF antigen expression. The ST3GAL1-transfected Jurkat cells reduced the AAL/AAGL binding activity (Figure 6A,B), and the viable cell ratio was increased from 55.3 to 64.4% (Figure 6C). These results directly addressed the role of the *O*-glycan of the 3′-sulfo-TF antigen in regulating cell susceptibility to AAL/AAGL.

HL60 had a low ratio between GAL3ST2 and ST3GAL1. To increase the ratio between GAL3ST2 and ST3GAL1, GAL3ST2 was overexpressed in HL60 cells by stable transfection. Because of the competition of GAL3ST2 and ST3GAL1 for the same site of the TF antigen, overexpressing GAL3ST2 in HL60 cells increased the 3′-sulfo-TF antigen expression. As shown in Figure 6D,E, the GAL3ST2-transfected HL60 cells showed an increased AAL/AAGL binding activity, and their antitumor activity was increased from 22.7 to 43.9% (Figure 6F). Similar results were also observed in HeLa cells. The GAL3ST2-transfected HeLa cells showed an increased AAL/AAGL binding and antiproliferative activity (Figure 6G−I). Next, we calculated the ratios between GAL3ST2 and ST3GAL1 in the control cells and in the related enzyme overexpressing cells of the three cell lines (Jurkat or -M, HL60 or -M, and HeLa or -M), after which we analyzed the correlation between these ratios and the binding of AAL/AAGL (Figure 6J) and inhibitory activity of AAL/AAGL (Figure 6K), respectively. The results showed that there was a high correlation between the ratios and the binding and the inhibitory activity. Our data suggested that the expression of the 3′-sulfo-TF antigen determines the apoptosis-inducing activity of AAL/AAGL and that the sensitive cell lines have high ratios between GAL3ST2 and ST3GAL1. These results suggest that AAL/AAGL may potentially serve as a 3′-sulfo-TF ligand for cancer diagnosis and for targeted therapy.

3. DISCUSSION

Lectins are glycan-binding proteins whose activities depend on the binding to specific carbohydrate structures.[20] To date, glycan ligands of many lectins have been identified by glycan arrays and other methods. These data have helped to develop many new methods for using lectins in glycan enrichment,

https://doi.org/10.1021/acsomega.1c01544
ACS Omega 2021, 6, 17379−17390

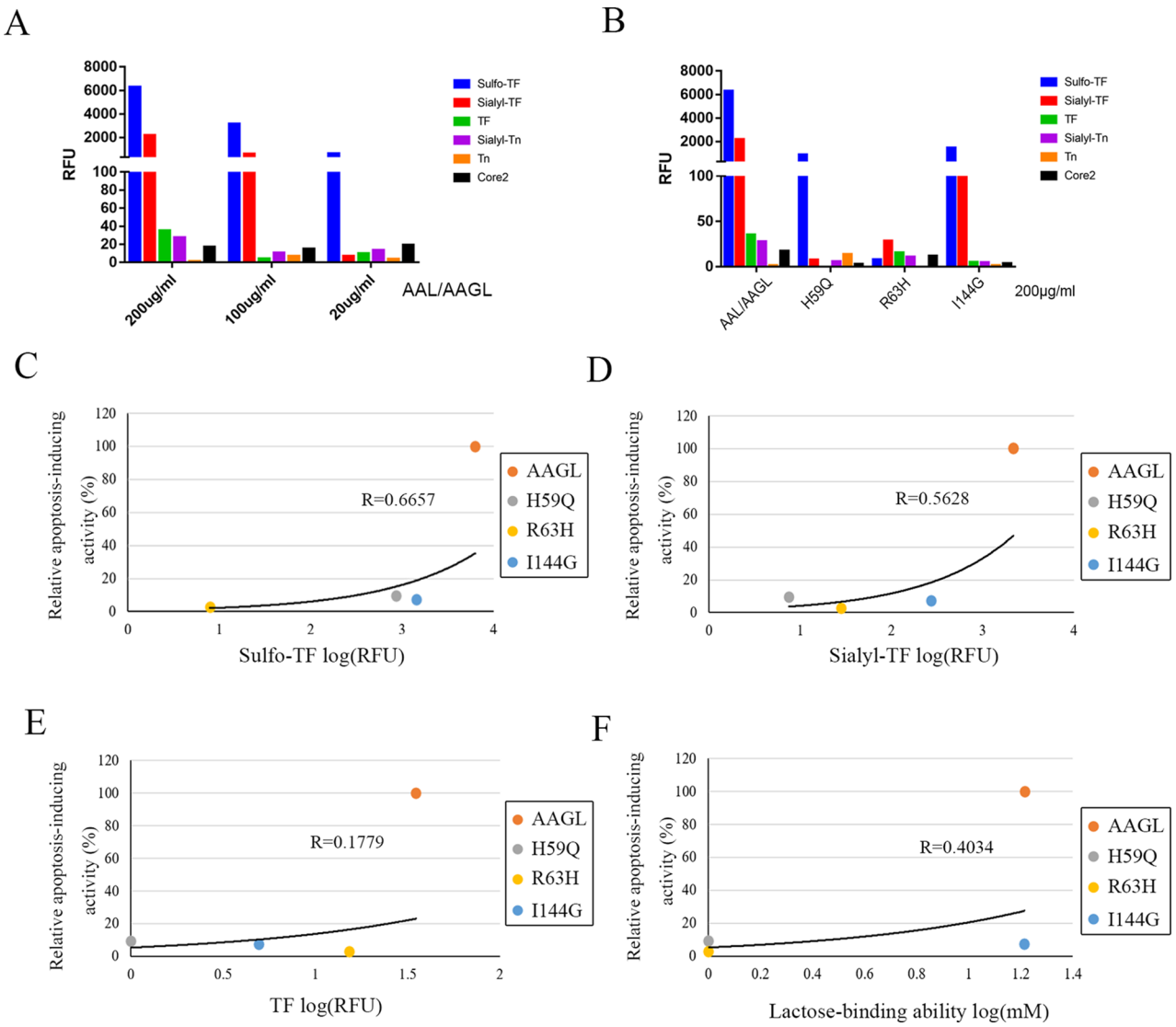

Figure 4. 3′-Sulfo-TF and 3′-sialyl-TF on the cell surface may determine the antitumor activity of AAL/AAGL. Glycan array analysis data. (A) Binding activity of AAL/AAGL (200, 100, and 20 μg/mL) to TF and related glycans. (B) Binding activity of AAL/AAGL and three AAL/AAGL mutants (R59Q, R63H, and I144G, 200 μg/mL) to TF and related glycans. RFU: relative fluorescence unit. (C) Linear regression analysis of binding activity to 3′-sulfo-TF and apoptosis-inducing activity of AAL/AAGL and three AAL/AAGL mutants, which showed an R value of 0.6657. (D) Linear regression analysis of binding activity to 3′-sialyl-TF and apoptosis-inducing activity of AAL/AAGL and three AAL/AAGL mutants, which showed an R value of 0.5628. (E) Linear regression analysis of binding activity to TF and apoptosis-inducing activity of AAL/AAGL and three AAL/AAGL mutants, which showed an R value of 0.1779. (F) Linear regression analysis of lactose-binding activity and apoptosis-inducing activity of AAL/AAGL and three AAL/AAGL mutants, which showed an *R* value of only 0.4034.

drug delivery, and even tumor therapy.[33] Glycan arrays provide valuable candidate glycan ligands of lectins. However, those candidate glycan ligands should be further verified because lectin may recognize different ligands in different cells or species. Our data indicated that AAL/AAGL recognizes 3′-sulfo-TF in human cells. However, the sialic acid-sugars (Figure S1) may be AAL/AAGL's ligands in *Agrocybe aegertia*, from which AAL/AAGL purified. Identifying the physiological ligands of lectins in cells needs more investigation, which is important for the more effective use of lectins. In this paper, based on the glycan array data, we successfully identified that 3′-sulfo-TF is one of the main ligands involved in the apoptosis-inducing activity of AAL/AAGL by analyzing glycosyltransferases. Our work provides a reference for the study of the physiological glycan ligands of other lectins.

AAL/AAGL is an edible mushroom lectin and belongs to the galectin family, which has a highly conserved CRD region that recognizes β-galactoside-containing glycans. Mammalian galectin has been intensively investigated for its ubiquitous location and for its ability to regulate multiple biologic functions.[34,35] Although there are some studies on glycan ligands of mammalian galectin that reported that LacNAc was a common ligand of all galectins,[36] it is obvious that galectins function with distinct activities through different glycans. The TF-related antigens (Gal1−3GalNAc1-Ser/Thr, Thomsen-Friedenreich, TF antigen) which are overexpressed at the tumor cell surface and have been proposed to facilitate tumor progression by helping tumor cells to escape from immunity and by protecting tumor cells from apoptosis.[37−39] It has been reported that Gal-2 could interact with mucin in a β-galactoside-dependent manner, strengthening the gastric

https://doi.org/10.1021/acsomega.1c01544
ACS Omega 2021, 6, 17379−17390

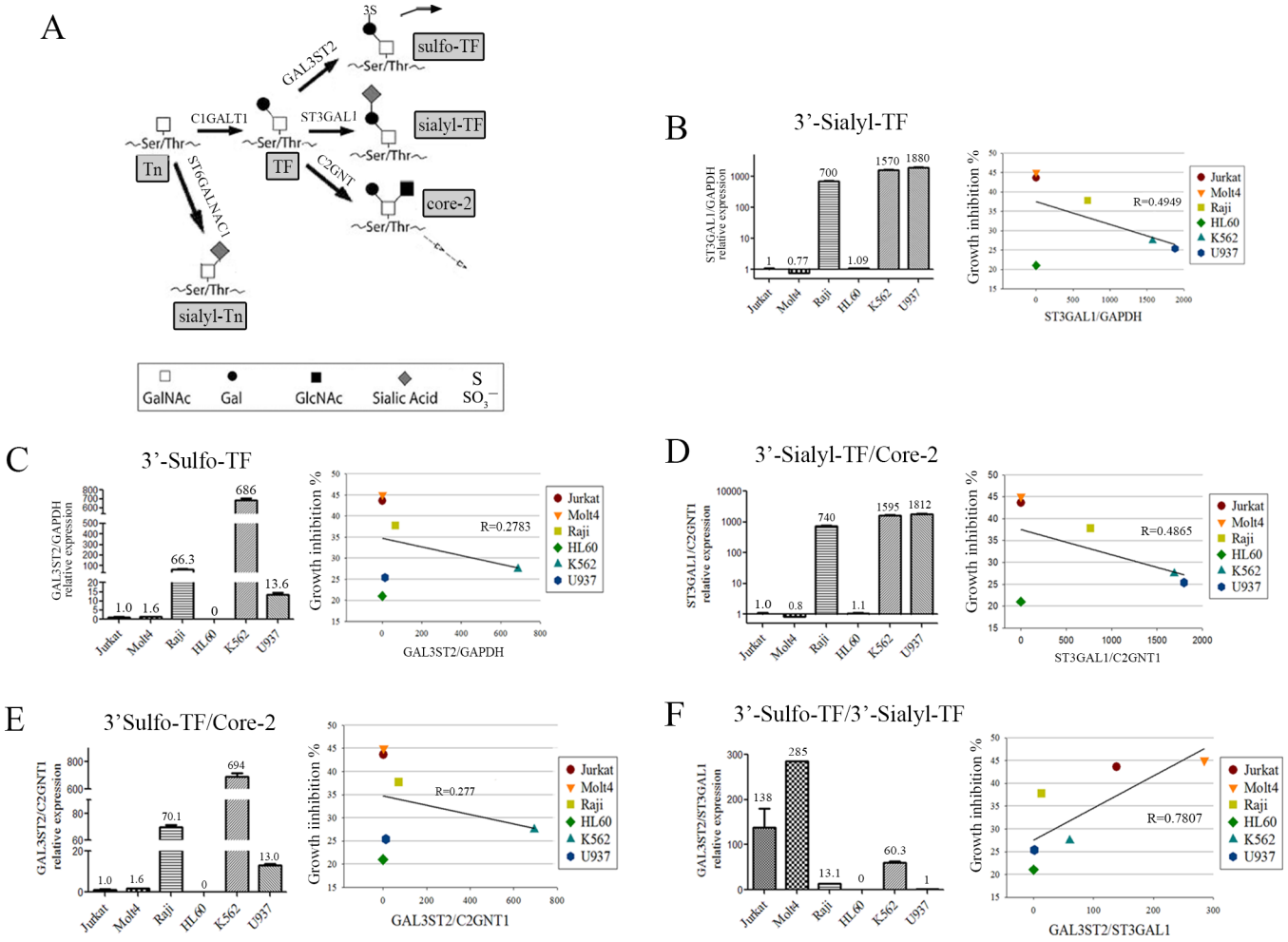

Figure 5. Antitumor activity of AAL/AAGL has a high-positive correlation with GAL3ST2/ST3GAL1 (indicate Sulfo-TF/Sialyl-TF). (A) Synthesis pathways of TF and its related antigens. The mRNA expression levels of (B) 3′-sialyl-TF synthesis enzyme ST3GAL1; (C) 3′-sulfo-TF synthesis enzyme GAL3ST2; (D) synthesis enzyme ratio of 3′-sialyl-TF/Core2; (E) synthesis enzyme ratio of 3′-sulfo-TF/Core2; (F) synthesis enzyme ratio of 3′-sulfo-TF/3′-sialyl-TF (GAL3ST2/ST3GAL1) was used to analyze the correlation with the tumor growth inhibition rate of AAL/AAGL.

Table 2. Relationships among the Expressions of Glycosyltransferases, Glycan Structures, and the AAL/AAGL Sensitivity of Cells

glycosyltransferase (normalized to GAPDH)	product	*R* value
C1GALT1	TF	0.2471
C2GNT1	core-2	0.6652
C2GNT2	core-2	0.3186
ST6GALNAC1	sialyl-Tn	0.465
ST3GAL1	3′-sialyl-TF	0.4949
GAL3ST2	3′-sulfo-TF	0.2783
GAL3ST2/C2GNT1	3′-sulfo-TF/core-2	0.277
ST3GAL1/C2GNT1	3′-sialyl-TF/core-2	0.4865
GAL3ST2/C1GALT1	3′-sulfo-TF/TF	0.2755
ST3GAL1/C1GALT1	3′-sialyl-TF/TF	0.4605
GAL3ST2/ST3GAL1	**3′-sulfo-TF/3′-sialyl-TF**	**0.7807**

mucosa barrier structure.[40] The crystal structure analysis supports the identification of the distinct TF-binding properties of Gal-1 and Gal-3.[41] It has been reported that core 2 *O*-glycans are receptors for galectin-1. Conversely, Gal-1 binding is thwarted when LacNAc is modified by a 2,3-linked sialic acid.[42] Core 2 *O*-glycans may be the primary ligands for Gal-3 on diffuse large B-cell lymphoma (DLBCL) cells as a novel mechanism of apoptosis resistance in DLBCL.[43]

The sulfation modification is an important event in cell adhesion, bacterial binding, and the regulation of biosynthetic pathways.[44,45] Sulfated glycoconjugates were found in a wide range of biological compounds, including glycoproteins, proteoglycans, glycolipids, and polysaccharides, which contribute to many important physiological processes, such as inflammatory reaction, blood coagulation, and cell adhesion and cancer metastasis.[46,47] When the TF antigen is catalyzed by GAL3ST2 at the C3 position of galactose, the 3′-sulfo-TF antigen ([3OSO3]-Galβ1−3GalNAcα-Ser/Thr) is produced.[37] In breast epithelial mammary tumors, GAL3ST2 is more strongly expressed in more metastatic tumors,[48,49] indicating that 3′-sulfo-TF expressed from tumor cells may be a promising prognostic marker. The 3′-sulfo-TF antigen is also identified as the ligand of Galectin-4,[50,51] a member of human galectin, which is expressed in the epithelium of the alimentary tract. Hiroko Ideo et al. showed that MUC1 possessing a 3′-sulfo-TF antigen was highly expressed in the blood streams of patients with recurrent and/or metastatic breast cancer. The Gal4/MUC1(3′-sulfo-TF) assay was more sensitive than the

https://doi.org/10.1021/acsomega.1c01544
ACS Omega 2021, 6, 17379−17390

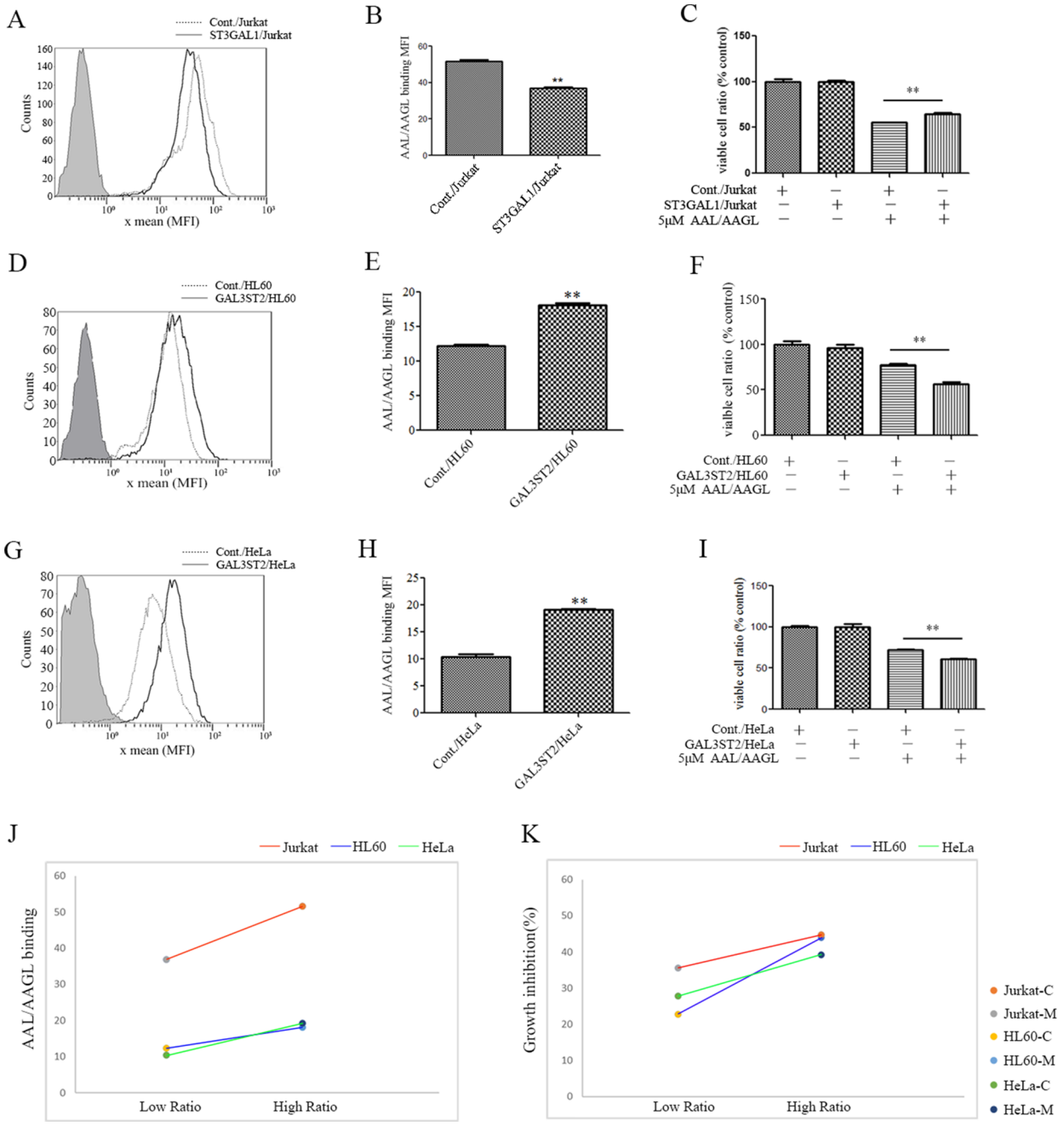

Figure 6. Ratio between GAL3ST2 and ST3GAL1 regulates the AAL/AAGL sensitivity of cells. (A) Affinities of Jurkat cells (solid line) overexpressing ST3GAL1, and the control Jurkat cells (dotted line) for AAL/AAGL were determined by flow cytometry after the cells were incubated with AAL/AAGL. (B) Statistics data of Figure 6A. (C) Analysis of the viable cell ratio of the Jurkat cells overexpressing ST3GAL1 and the control Jurkat cells that were treated with AAL/AAGL. (D, E) Binding of HL60 cells (solid line) overexpressing GAL3ST2 and the control HL60 cells (dotted line) for AAL/AAGL. (F) Analysis of the viable cell ratio of the GAL3ST2-overexpressing HL60 cells and control HL60 cells that were treated with AAL/AAGL. (G–I) Treatment of the HeLa cells was the same as that for the HL60 cells as mentioned above, and GAL3ST2 was overexpressed in the HeLa cells. $^{**}p < 0.01$. (J, K) Ratio of GAL3ST2 to ST3GAL1 before and after the overexpression of glycosyltransferases in three cell lines (Jurkat, HL60, and HeLa cells) was correlated with the (J) AAL/AAGL binding and (K) growth inhibition rate of the cells.

cancer antigen15−3 assay, especially in the relapsed or metastatic breast cancer.[52] Galectin-4 suppresses T cell activation depended on the 3′-sulfo-glycolipid group.[53] Galectin-4 could be used as for the quantification of the 3′-sulfo-TF antigen on account of high binding affinity to it. In this report, we identified 3′-sulfo-TF as the glycan ligand of AAL/AAGL and showed the expression of the 3′-sulfo-TF antigen, which is determined by the ratio of GAL3ST2/ST3GAL1. This work also suggests that AAL/AAGL potentially could be used for cancer diagnosis, therapy, and quantification of the 3′-sulfo-TF antigen.

Recently, some lectins have the ability to discriminate between normal cells and tumor cells as a result of their different glycosylation patterns. The use of lectins in the modification of nanoparticles for anticancer drug delivery has been reported.[54] The plant lectin ConA covalently coupled with nanoparticles has been developed for bone cancer treatment.[55] G. Obaid, I et al. showed that jacalin, a lectin

https://doi.org/10.1021/acsomega.1c01544
ACS Omega 2021, 6, 17379−17390

specific for the T antigen, can deliver nanoparticles to HT-29 human colon adenocarcinoma cells.[56] These new pharmaceutical preparations increase antitumor effectiveness and decrease toxicity toward healthy cells. AAL/AAGL with high binding affinity to the 3′-sulfo-TF antigen could be covalently coupled with nanoparticles and emerged as important tools to target cancer therapy.

Of note, even though galectins recognize similar glycosidic structures, different galectins can induce distinct or even opposite activities.[35] It should be considered that galectins could exert diverse activities through slightly different glycans on different types of cells or under stimulation. In addition to antitumor activity, AAL/AAGL has also been reported to play important roles in fungus development from mycelia to the fruiting body.[57] In this report, we found that the glycan ligand of *O*-glycan (3′-sulfo-TF) was the glycan ligand for AAL/AAGL antitumor activity, but there may be other glycan ligands for AAL/AAGL's multiple functions that remain unknown and deserve further investigation.

4. MATERIALS AND METHODS

4.1. Glycan Array Analysis. A complete list of the glycans and the RFU values obtained for the binding of AAL/AAGL (200, 100, and 20 μg/mL) and several mutants (200 μg/mL) (Supporting data1−6), along with the statistical analysis, is available at http://www.functionalglycomics.org/ by searching the lectin name "AAL."

4.2. Cell Lines and Reagents. Human leukemia cell lines derived from acute myelogenous leukemia (HL-60), erythroblastic cell leukemia (K562), pro-monocytic leukemia (U937), Burkitt's lymphoma (Raji), and T-cell leukemia (Molt-4, Jurkat) were obtained from the CCTCC (China Center for Type Culture Collection, Wuhan, Huibei, People's Republic of China). All cells were grown in the RPMI medium supplemented with fetal bovine serum, 100 mg/mL streptomycin, and 100 units/mL penicillin. Recombinant AAL/AAGL was purified as previously described.[58]

4.3. Assays for Growth Inhibition and Apoptosis. Cells were treated with 5 μM AAL/AAGL, 100 μM lactose, and 50 μM Z-VAD-FMK or with appropriate buffer controls for 48 h at 37 °C. The growth-inhibitory effect of AAL/AAGL was then analyzed with a modified MTT assay using the Cell Counting Kit-8 (Dojindo, Japan). The data represent the results of the means±standard errors of three independent experiments. To assess apoptosis, the cells were counterstained with propidium iodide and annexin V-FITC.

4.4. Western Blotting. Western blotting was performed as described previously. The primary antibodies (Abs) used were those against caspase-3, poly (ADP-ribose) polymerase (PARP), phosphorylated JNK (all from Cell Signaling Technology, Beverly, MA, USA), the TF antigen (A78-G/A7), actin, β-tubulin (all from Santa Cruz Biotechnology, Santa Cruz, CA, USA), caspase-9, caspase-8, bcl-2, GAPDH (all from Beyotime Institute of Biotechnology, Jiangsu, Haimen, China), and FAS (Proteintech Group, Chicago, IL, USA).

4.5. Cell Surface Binding Affinity of AAL/AAGL. Cells were treated with 2 mM benzyl-a-GalNAc in ethanol or with appropriate buffer controls for 72 h at 37 °C. Cells (1×10^6) were incubated with AAL/AAGL (5 μM) in PBS buffer containing 5.0% BSA. After being washed in PBS, the cells were incubated with a polyclonal rabbit anti-AAL/AAGL antibody (1:100) for 1 h, after which a FITC-conjugated goat antirabbit IgG (Pierce Chemical Co., Rockford, IL, USA) was added to the sample and incubated for 30 min followed by washing with PBS. For the negative control, the cells were incubated only with the polyclonal rabbit anti-AAL/AAGL antibody and the FITC-conjugated goat antirabbit antibody. After binding of AAL/AAGL, the stably transfected cells were finally stained with Texas red-conjugated goat antirabbit antibody. The cells were washed twice and subjected to flow cytometric analysis. Statistical software GraphPad Prism was used for ANOVA analysis of flow cytometry data. All treatments were performed three times.

4.6. Analysis of Glycosyltransferase Gene Expression. RNA was isolated as described previously.[59] RT-PCR was performed according to the protocol provided in the SuperScript One-Step RT-PCR with Platinum Taq (Invitrogen). The real-time PCR of core 1 synthase (C1GALT1), glucosaminyl (*N*-acetyl) transferase 1 (C2GNT1), C2GNT2, ST3 beta-galactoside alpha-2,3-sialyltransferase 1 (ST3GAL1), alpha-*N*-acetylgalactosaminide alpha-2,6-sialyltransferase 1 (ST6GALNAC1), and galactose-3-O-sulfotransferase 2 (GAL3ST2) was performed. Quantitation of human glycosyltransferase transcript expression by real-time PCR was performed on a real-time PCR detection system with SYBR Green Real-time PCR Master Mix (TOYOBO, Japan) using 1 μL of cDNA. The PCR conditions included 1 cycle at 95 °C for 2 min followed by 45 cycles at 95 °C for 15 s, 60 °C for 15 s, and 72 °C for 45 s. The amount of glycosyltransferase transcript was normalized to the amount of GAPDH transcript in the same cDNA sample. Relative fold differences in transcript expression were approximated using the comparative CT method. Real-time PCR was performed using the following PCR primers: C1GALT1, 5-TCATCCCTTTGTGCCAGAACACC-3 (5′-primer) and 5-TCAGAGCAGCAACCAGGACCCTC-3 (3′-primer); C2GNT1, 5-GACGTTGCTGCGAAGG-3 (5′-primer) and 5- CCAAGTGTCTGACACTTACA-3 (3′-primer); C2GNT2 5-GGCAGTGCTTCAGGCTATTC-3 (5′-primer) and 5-GGCATACACAGCTCGCAGTA-3 (3′-primer); ST3GAL1, 5-ATGCATGTCTGCGATGAGGTGGACTTGT-3 (5′-primer) and 5-GCCAAGGTGGCCGTCACGTTAGACT-3 (3′-primer); ST6GALNAC1; GAL3ST2, 5-TGTTCCTGAAGACGCACAAG-3 (5′-primer) and 5-AACCTCAGGTGGTTGCACAT-3 (3′-primer). To validate differences in the expression levels of ST3GAL1 and the C2GNT2, reverse transcription-PCR (RT-PCR) analysis was performed. Semi-quantitative PCR was performed using the following PCR primers: ST3GAL1, 5-CTCACCTCCTTCTTCCTGAACTACT-3 (5′-primer) and ST3GAL1, 5-GACAAAGTCGTGACTGTCTATCTCA-3 (3′-primer); GAL3ST2, 5-AGAGATACTTCCGGGTCATCCTC-3 (5′-primer) and GAL3ST2, 5-GCGTAGGTTTTGTAGTAGATGAAGG-3 (3′-primer); GAPDH, 5-AGGTCGGAGTCAACGGATTTG-3 (5′-primer) and GAPDH, 5-GTGATGGCATGGACTGTGGT-3 (3′-primer).

4.7. Expression of β-Galactoside α2,3-Sialyltransferase 1 in Jurkat Cells. β-Galactoside α2,3-sialyltransferase 1 (ST3GAL1) cDNA (gift of Dr. Linda G. Baum, Department of Pathology and Laboratory Medicine, School of Medicine, University of California at Los Angeles) was subcloned into pEGFP (Clontech; pST3). Jurkat cells (2×10^7) were transfected with 100 μg of pST3 or vector alone (control) by electroporation. Stable transfectants were isolated using 0.8 mg/mL G418 (Sigma). Clones appeared after 3 weeks and

https://doi.org/10.1021/acsomega.1c01544
ACS Omega 2021, 6, 17379−17390

were selected according to their phenotype as determined by FACS analysis.

4.8. Expression of Galactose-3-O-Sulfotransferase 2 in HL60 Cells. Galactose-3-O-sulfoTransferase 2 (GAL3ST2) cDNA (gift of Dr. Koichi Honke, Department of Biochemistry, Kochi University Medical School, Kohasu, Japan) was subcloned into pEGFP (Clontech; pST3). HL60 cells (2×10^7) were transfected with 100 μg of pST3 or vector alone (control) by electroporation. Stable transfectants were isolated using 0.8 mg/mL G418 (Sigma). Clones appeared after 3 weeks and were selected according to their phenotype as determined by FACS analysis.

4.9. Chemicals. Z-VAD-FMK was purchased from the Beyotime Institute of Biotechnology (Jiangsu, Haimen, China); benzyl-a-*N*-acetylgalactosamine (benzyl-a-GalNAc), G418, and lactose were purchased from Sigma (St Louis, MO, USA).

■ ASSOCIATED CONTENT

Supporting Information

The Supporting Information is available free of charge at https://pubs.acs.org/doi/10.1021/acsomega.1c01544.

The mRNA expression levels of several glycosyltransferases and the glycan array data of AAGL and mutation (R63H, H59Q, and I144G) (PDF)

■ AUTHOR INFORMATION

Corresponding Authors

Yijie Chen − *College of Food Science and Technology, Huazhong Agricultural University, Wuhan, Hubei Province 430070, P. R. China;* orcid.org/0000-0001-9477-5058; Email: yijiechen@mail.hzau.edu.cn

Hui Sun − *, Wuhan, Hubei Province 430072, P. R. China; Hubei Province key Laboratory of Allergy and Immunology, Wuhan University, Wuhan, Hubei Province 430072, P. R. China;* orcid.org/0000-0001-9275-9257; Email: sunhui@whu.edu.cn

Authors

Yang Li − *, Wuhan, Hubei Province 430072, P. R. China*

Yan Li − *, Wuhan, Hubei Province 430072, P. R. China*

Jing Xia − *, Wuhan, Hubei Province 430072, P. R. China*

Qing Yang − *College of Food Science and Engineering, Wuhan Polytechnic University, Wuhan, Hubei Province 430023, P. R. China*

Complete contact information is available at: https://pubs.acs.org/10.1021/acsomega.1c01544

Funding

This research was supported by the National Natural Science Foundation of China. Author Hui Sun received funding from NSFC Grant 81670531, 31972019, and 31800676.

Notes

The authors declare no competing financial interest.

■ ACKNOWLEDGMENTS

We would like to acknowledge Dr. Linda G Baum and Dr. Koichi Honke for providing us with the cDNA of ST3GAL1 and GAL3ST2, respectively. We thank Dr. Akira Seko and Dr. Yamashita for assistance during experiments.

■ ABBREVIATIONS USED

AAL/AAGLtab*Agrocybe aegerita* lectin
TF antigentabThomsen-Friedenreich antigen
ConAtabConcanavalin A
PHAtab*Phaseolus vulgaris* agglutinin
AGGtabAbrus agglutinin
RCA Itab*Ricinus communis* agglutinin I
PHA-Etab*Phaseolus vulgaris* lectin
C1GALT1tabcore 1 synthase
C2GNT1tabcore-2 β1−6-*N*-acetylglucosaminyl transferase 1
ST3GAL1tabST3 beta-galactoside alpha-2,3-sialyltransferase 1
ST6GALNAC1tabalpha-*N*-acetylgalactosaminide alpha-2,6-sialyltransferase 1;
GAL3ST2tabgalactose-3-*O*-sulfotransferase 2
ST6GAL1tabalpha 2,6 sialyltransferase 1
DLBCLtabdiffuse large B-cell lymphoma
FBStabfetal bovine serum

■ REFERENCES

(1) De Mejia, E. G.; Prisecaru, V. I. Lectins as bioactive plant proteins: a potential in cancer treatment. *Crit. Rev. Food Sci. Nutr.* **2005**, *45*, 425−445.

(2) Swanson, M. D.; Boudreaux, D. M.; Salmon, L.; Chugh, J.; Winter, H. C.; Meagher, J. L.; Andre, S.; Murphy, P. V.; Oscarson, S.; Roy, R.; King, S.; Kaplan, M. H.; Goldstein, I. J.; Tarbet, E. B.; Hurst, B. L.; Smee, D. F.; de la Fuente, C.; Hoffmann, H. H.; Xue, Y.; Rice, C. M.; Schols, D.; Garcia, J. V.; Stuckey, J. A.; Gabius, H. J.; Al-Hashimi, H. M.; Markovitz, D. M. Engineering a therapeutic lectin by uncoupling mitogenicity from antiviral activity. *Cell* **2015**, *163*, 746−758.

(3) van Eijk, M.; Rynkiewicz, M. J.; Khatri, K.; Leymarie, N.; Zaia, J.; White, M. R.; Hartshorn, K. L.; Cafarella, T. R.; van Die, I.; Hessing, M.; Seaton, B. A.; Haagsman, H. P. Lectin-mediated binding and sialoglycans of porcine surfactant protein D synergistically neutralize influenza A virus. *J. Biol. Chem.* **2018**, *293*, 10646−10662.

(4) Elola, M. T.; Blidner, A. G.; Ferragut, F.; Bracalente, C.; Rabinovich, G. A. Assembly, organization and regulation of cell-surface receptors by lectin-glycan complexes. *Biochem. J.* **2015**, *469*, 1−16.

(5) Fuster, M. M.; Esko, J. D. The sweet and sour of cancer: Glycans as novel therapeutic targets. *Nat. Rev. Cancer* **2005**, *5*, 526−542.

(6) Shi, Z.; Li, W. W.; Tang, Y.; Cheng, L. J. A Novel Molecular Model of Plant Lectin-Induced Programmed Cell Death in Cancer. *Biol. Pharm. Bull.* **2017**, *40*, 1625−1629.

(7) Bhutia, S. K.; Panda, P. K.; Sinha, N.; Praharaj, P. P.; Bhol, C. S.; Panigrahi, D. P.; Mahapatra, K. K.; Saha, S.; Patra, S.; Mishra, S. R.; Behera, B. P.; Patil, S.; Maiti, T. K. Plant lectins in cancer therapeutics: Targeting apoptosis and autophagy-dependent cell death. *Pharmacol. Res.* **2019**, *144*, 8−18.

(8) Lai, Y. C.; Chuang, Y. C.; Chang, C. P.; Yeh, T. M. Macrophage migration inhibitory factor has a permissive role in concanavalin A-induced cell death of human hepatoma cells through autophagy. *Cell Death Dis.* **2015**, *6*, No. e2008.

(9) Pryme, I. F.; Bardocz, S.; Pusztai, A.; Ewen, S. W. B. The growth of an established murine non-Hodgkin lymphoma tumour is limited by switching to a phytohaemagglutinin-containing diet. *Cancer Lett.* **1999**, *146*, 87−91.

(10) Han, S. Y.; Hong, C. E.; Kim, H. G.; Lyu, S. Y. Anti-cancer effects of enteric-coated polymers containing mistletoe lectin in murine melanoma cells in vitro and in vivo. *Mol. Cell. Biochem.* **2015**, *408*, 73−87.

(11) Panda, P. K.; Naik, P. P.; Praharaj, P. P.; Meher, B. R.; Gupta, P. K.; Verma, R. S.; Maiti, T. K.; Shanmugam, M. K.; Chinnathambi, A.; Alharbi, S. A.; Sethi, G.; Agarwal, R.; Bhutia, S. K. Abrus agglutinin

stimulates BMP-2-dependent differentiation through autophagic degradation of -catenin in colon cancer stem cells. *Mol. Carcinogen.* **2018**, *57*, 664−677.
(12) Sinha, N.; Panda, P. K.; Naik, P. P.; Das, D. N.; Mukhopadhyay, S.; Maiti, T. K.; Shanmugam, M. K.; Chinnathambi, A.; Zayed, M. E.; Alharbi, S. A.; Sethi, G.; Agarwal, R.; Bhutia, S. K. Abrus agglutinin promotes irreparable DNA damage by triggering ROS generation followed by ATM-p73 mediated apoptosis in oral squamous cell carcinoma. *Mol. Carcinog.* **2017**, *56*, 2400−2413.
(13) Fang, E. F.; Zhang, C. Z. Y.; Ng, T. B.; Wong, J. H.; Pan, W. L.; Ye, X. J.; Chan, Y. S.; Fong, W. P. Momordica Charantia lectin, a type II ribosome inactivating protein, exhibits antitumor activity toward human nasopharyngeal carcinoma cells in vitro and in vivo. *Cancer Prev. Res. (Phila)* **2012**, *5*, 109−121.
(14) You, W. K.; Kasman, I.; Hu-Lowe, D. D.; McDonald, D. M. Ricinus communis agglutinin I leads to rapid down-regulation of VEGFR-2 and endothelial cell apoptosis in tumor blood vessels. *Am. J. Pathol.* **2010**, *176*, 1927−1940.
(15) Steele, M. L.; Axtner, J.; Happe, A.; Kroz, M.; Matthes, H.; Schad, F. Use and Safety of Intratumoral Application of European Mistletoe (Viscum album L) Preparations in Oncology. *Integr. Cancer Ther.* **2015**, *14*, 140−148.
(16) von Schoen-Angerer, T.; Goyert, A.; Vagedes, J.; Kiene, H.; Merckens, H.; Kienle, G. S. Disappearance of an advanced adenomatous colon polyp after intratumoural injection with Viscum album (European mistletoe) extract: a case report. *J. Gastrointestin. Liver Dis.* **2014**, *23*, 449−452.
(17) Schad, F.; Thronicke, A.; Steele, M. L.; Merkle, A.; Matthes, B.; Grah, C.; Matthes, H. Overall survival of stage IV non-small cell lung cancer patients treated with Viscum album L. in addition to chemotherapy, a real-world observational multicenter analysis. *PLoS One* **2018**, *13*, No. e0203058.
(18) Semiglazov, V. F.; Stepula, V. V.; Dudov, A.; Schnitker, J.; Mengs, U. Quality of life is improved in breast cancer patients by standardised mistletoe extract PS76A2 during chemotherapy and follow-up: A randomised, placebo-controlled, double-blind, multi-centre clinical trial. *Anticancer Res.* **2006**, *26*, 1519−1529.
(19) de Oliveira Figueiroa, E.; Albuquerque da Cunha, C. R.; Albuquerque, P. B. S.; de Paula, R. A.; Aranda-Souza, M. A.; Alves, M. S.; Zagmignan, A.; Carneiro-da-Cunha, M. G.; Nascimento da Silva, L. C.; Dos Santos Correia, M. T. Lectin-Carbohydrate Interactions: Implications for the Development of New Anticancer Agents. *Curr. Med. Chem.* **2017**, *24*, 3667−3680.
(20) Kaltner, H.; Abad-Rodriguez, J.; Corfield, A. P.; Kopitz, J.; Gabius, H. J. The sugar code: letters and vocabulary, writers, editors and readers and biosignificance of functional glycan-lectin pairing. *Biochem. J.* **2019**, *476*, 2623−2655.
(21) Tian, D. R.; Zhang, L.; Zhang, S.; Kong, X. W.; Sheng, K. L.; Wang, J. M.; Zhang, M.; Wang, Y. Z. Heterologous expression and molecular binding properties of AofleA, a fucose-specific lectin from nematophagous fungus Arthrobotrys oligospora. *Int. J. Biol. Macromol.* **2020**, *149*, 1213−1221.
(22) Christie, M. P.; Toth, I.; Simerská, P. Biophysical characterization of lectin-glycan interactions for therapeutics, vaccines and targeted drug delivery. *Future Med. Chem.* **2014**, *6*, 2113−2129.
(23) Venkataraman, M.; Sasisekharan, R.; Raman, R. Glycan array data management at Consortium for Functional Glycomics. *Methods Mol. Biol.* **2015**, *1273*, 181−190.
(24) Abbott, K. L.; Pierce, J. M. Lectin-based glycoproteomic techniques for the enrichment and identification of potential biomarkers. *Methods Enzymol.* **2010**, *480*, 461−476.
(25) Tremblay, R.; Feng, M.; Menassa, R.; Huner, N. P. A.; Jevnikar, A. M.; Ma, S. W. High-yield expression of recombinant soybean agglutinin in plants using transient and stable systems. *Transgenic Res.* **2011**, *20*, 345−356.
(26) Nagae, M.; Soga, K.; Morita-Matsumoto, K.; Hanashima, S.; Ikeda, A.; Yamamoto, K.; Yamaguchi, Y. Phytohemagglutinin from Phaseolus vulgaris (PHA-E) displays a novel glycan recognition mode using a common legume lectin fold. *Glycobiology* **2014**, *24*, 368−378.
(27) Unitt, J.; Hornigold, D. Plant lectins are novel Toll-like receptor agonists. *Biochem. Pharmacol.* **2011**, *81*, 1324−1328.
(28) Liang, Y.; Feng, L.; Tong, X.; Wang, K.; Li, D. F.; Lin, J. C.; Tang, Z. J.; Liu, H. H.; Jiang, S.; Guo, L.; Wang, D. C.; Sun, H. Importance of nuclear localization for the apoptosis-induced activity of a fungal galectin AAL (Agrocybe aegerita lectin). *Biochem. Biophys. Res. Commun.* **2009**, *386*, 437−442.
(29) Liang, Y.; Lin, J. C.; Wang, K.; Chen, Y. J.; Liu, H. H.; Luan, R.; Jiang, S.; Che, T.; Zhao, Y.; Li, D. F.; Wang, D. C.; Guo, L.; Sun, H. A nuclear ligand MRG15 involved in the proapoptotic activity of medicinal fungal galectin AAL (Agrocybe aegerita lectin). *Bba-Gen Subjects* **2010**, *1800*, 474−480.
(30) Yang, N.; Li, D. F.; Feng, L.; Xiang, Y.; Liu, W.; Sun, H.; Wang, D. C. Structural basis for the tumor cell apoptosis-inducing activity of an antitumor lectin from the edible mushroom Agrocybe aegerita. *J. Mol. Biol.* **2009**, *387*, 694−705.
(31) Feng, L.; Sun, H.; Zhang, Y.; Li, D. F.; Wang, D. C. Structural insights into the recognition mechanism between an antitumor galectin AAL and the Thomsen-Friedenreich antigen. *Faseb J.* **2010**, *24*, 3861−3868.
(32) Zhao, C. G.; Sun, H.; Tong, X.; Qi, Y. P. An antitumour lectin from the edible mushroom Agrocybe aegerita. *Biochem. J.* **2003**, *374*, 321−327.
(33) Syed, P.; Gidwani, K.; Kekki, H.; Leivo, J.; Pettersson, K.; Lamminmaki, U. Role of lectin microarrays in cancer diagnosis. *Proteomics* **2016**, *16*, 1257−1265.
(34) Giovannone, N.; Smith, L. K.; Treanor, B.; Dimitroff, C. J. Galectin-Glycan Interactions as Regulators of B Cell Immunity. *Front Immunol.* **2018**, *9*, 2839.
(35) Nielsen, M. I.; Stegmayr, J.; Grant, O. C.; Yang, Z.; Nilsson, U. J.; Boos, I.; Carlsson, M. C.; Woods, R. J.; Unverzagt, C.; Leffler, H.; Wandall, H. H. Galectin binding to cells and glycoproteins with genetically modified glycosylation reveals galectin-glycan specificities in a natural context. *J. Biol. Chem.* **2018**, *293*, 20249−20262.
(36) Xiao, Q.; Ludwig, A. K.; Romano, C.; Buzzacchera, I.; Sherman, S. E.; Vetro, M.; Vertesy, S.; Kaltner, H.; Reed, E. H.; Moller, M.; Wilson, C. J.; Hammer, D. A.; Oscarson, S.; Klein, M. L.; Gabius, H. J.; Percec, V. Exploring functional pairing between surface glycoconjugates and human galectins using programmable glycodendrimersomes. *Proc. Natl. Acad. Sci. U. S. A.* **2018**, *115*, E2509−E2518.
(37) Sindrewicz, P.; Lian, L. Y.; Yu, L. G. Interaction of the Oncofetal Thomsen-Friedenreich Antigen with Galectins in Cancer Progression and Metastasis. *Front. Oncol.* **2016**, *6*, 79.
(38) Inamdar, S. R.; Savanur, M. A.; Eligar, S. M.; Chachadi, V. B.; Nagre, N. N.; Chen, C.; Barclays, M.; Ingle, A.; Mahajan, P.; Borges, A.; Shastry, P.; Kalraiya, R. D.; Swamy, B. M.; Rhodes, J. M.; Yu, L. G. The TF-antigen binding lectin from Sclerotium rolfsii inhibits growth of human colon cancer cells by inducing apoptosis in vitro and suppresses tumor growth in vivo. *Glycobiology* **2012**, *22*, 1227−1235.
(39) Chentoufi, A. A.; Nesburn, A. B.; BenMohamed, L. Recent advances in multivalent self adjuvanting glycolipopeptide vaccine strategies against breast cancer. *Arch. Immunol. Ther. Exp.* **2009**, *57*, 409−423.
(40) Tamura, M.; Sato, D.; Nakajima, M.; Saito, M.; Sasaki, T.; Tanaka, T.; Hatanaka, T.; Takeuchi, T.; Arata, Y. Identification of Galectin-2-Mucin Interaction and Possible Formation of a High Molecular Weight Lattice. *Biol. Pharm. Bull.* **2017**, *40*, 1789−1795.
(41) Bian, C. F.; Zhang, Y.; Sun, H.; Li, D. F.; Wang, D. C. Structural Basis for Distinct Binding Properties of the Human Galectins to Thomsen-Friedenreich Antigen. *PLoS One* **2011**, *6*, No. e25007.
(42) Valenzuela, H. F.; Pace, K. E.; Cabrera, P. V.; White, R.; Porvari, K.; Kaija, H.; Vihko, P.; Baum, L. G. O-glycosylation regulates LNCaP prostate cancer cell susceptibility to apoptosis induced by galectin-1. *Cancer Res.* **2007**, *67*, 6155−6162.
(43) Clark, M. C.; Pang, M.; Hsu, D. K.; Liu, F. T.; de Vos, S.; Gascoyne, R. D.; Said, J.; Baum, L. G. Galectin-3 binds to CD45 on

https://doi.org/10.1021/acsomega.1c01544
ACS Omega 2021, 6, 17379−17390

diffuse large B-cell lymphoma cells to regulate susceptibility to cell death. *Blood* **2012**, *120*, 4635−4644.
(44) Flowers, S. A.; Ali, L.; Lane, C. S.; Olin, M.; Karlsson, N. G. Selected reaction monitoring to differentiate and relatively quantitate isomers of sulfated and unsulfated core 1 O-glycans from salivary MUC7 protein in rheumatoid arthritis. *Mol. Cell. Proteomics* **2013**, *12*, 921−931.
(45) Yu, S. Y.; Hsiao, C. T.; Izawa, M.; Yusa, A.; Ishida, H.; Nakamura, S.; Yagi, H.; Kannagi, R.; Khoo, K. H. Distinct substrate specificities of human GlcNAc-6-sulfotransferases revealed by mass spectrometry-based sulfoglycomic analysis. *J. Biol. Chem.* **2018**, *293*, 15163−15177.
(46) Honke, K.; Taniguchi, N. Sulfotransferases and sulfated oligosaccharides. *Med. Res. Rev.* **2002**, *22*, 637−654.
(47) Kawashima, H.; Fukuda, M. J. A. Sulfated glycans control lymphocyte homing. *Ann. N. Y. Acad. Sci.* **2012**, *1253*, 112−121.
(48) Guerra, L. N.; Suarez, C.; Soto, D.; Schiappacasse, A.; Sapochnik, D.; Sacca, P.; Piwien-Pilipuk, G.; Peral, B.; Calvo, J. C. GAL3ST2 from mammary gland epithelial cells affects differentiation of 3T3-L1 preadipocytes. *Clin. Transl. Oncol.* **2015**, *17*, 511−520.
(49) Shi, B. Z.; Hu, P.; Geng, F.; He, P. J.; Wu, X. Z. Gal3ST-2 involved in tumor metastasis process by regulation of adhesion ability to selectins and expression of integrins. *Biochem. Biophys. Res. Commun.* **2005**, *332*, 934−940.
(50) Ideo, H.; Seko, A.; Ohkura, T.; Matta, K. L.; Yamashita, K. High-affinity binding of recombinant human galectin-4 to SO3–> 3Gal beta 1 -> 3GalNAc pyranoside. *Glycobiology* **2002**, *12*, 199−208.
(51) Vokhmyanina, O. A.; Rapoport, E. M.; Andre, S.; Severov, V. V.; Ryzhov, I.; Pazynina, G. V.; Korchagina, E.; Gabius, H. J.; Bovin, N. V. Comparative study of the glycan specificities of cell-bound human tandem-repeat-type galectin-4,-8 and-9. *Glycobiology* **2012**, *22*, 1207−1217.
(52) Ideo, H.; Hinoda, Y.; Sakai, K.; Hoshi, I.; Yamamoto, S.; Oka, M.; Maeda, K.; Maeda, N.; Hazama, S.; Amano, J.; Yamashita, K. Expression of mucin 1 possessing a 3-sulfated core1 in recurrent and metastatic breast cancer. *Int. J. Cancer* **2015**, *137*, 1652−1660.
(53) Mycko, M. P.; Sliwinska, B.; Cichalewska, M.; Cwiklinska, H.; Raine, C. S.; Selmaj, K. W. Brain Glycolipids Suppress T Helper Cells and Inhibit Autoimmune Demyelination. *J. Neurosci.* **2014**, *34*, 8646−8658.
(54) Ghazarian, H.; Idoni, B.; Oppenheimer, S. B. A glycobiology review: Carbohydrates, lectins and implications in cancer therapeutics. *Acta Histochem.* **2011**, *113*, 236−247.
(55) Martínez-Carmona, M.; Lozano, D.; Colilla, M.; Vallet-Regí, M. Lectin-conjugated pH-responsive mesoporous silica nanoparticles for targeted bone cancer treatment. *Acta Biomater.* **2018**, *65*, 393−404.
(56) Obaid, G.; Chambrier, I.; Cook, M. J.; Russell, D. A. Targeting the Oncofetal Thomsen-Friedenreich Disaccharide Using Jacalin-PEG Phthalocyanine Gold Nanoparticles for Photodynamic Cancer Therapy. *Angew. Chem., Int. Ed.* **2012**, *51*, 6158−6162.
(57) Luan, R.; Liang, Y.; Chen, Y.; Liu, H.; Jiang, S.; Che, T.; Wong, B.; Sun, H. Opposing developmental functions of Agrocybe aegerita galectin (AAL) during mycelia differentiation. *Fungal. Biol.* **2010**, *114*, 599−608.
(58) Yang, N.; Tong, X.; Xiang, Y.; Zhang, Y.; Sun, H.; Wang, D. C. Crystallization and preliminary crystallographic studies of the recombinant antitumour lectin from the edible mushroom Agrocybe aegerita. *Bba-Proteins Proteom.* **2005**, *1751*, 209−212.
(59) Barthel, S. R.; Gavino, J. D.; Wiese, G. K.; Jaynes, J. M.; Siddiqui, J.; Dimitroff, C. J. Analysis of glycosyltransferase expression in metastatic prostate cancer cells capable of rolling activity on microvascular endothelial (E)-selectin. *Glycobiology* **2008**, *18*, 806−817.

https://doi.org/10.1021/acsomega.1c01544
ACS Omega 2021, 6, 17379−17390